A Parameter Optimization to Solve the Inverse Problem in Electrocardiography

Gwladys Ravon, Rémi Dubois, Yves Coudière, Mark Potse

A parameter optimization to solve the inverse problem in electrocardiography

Gwladys Ravon[1,2,3*], Rémi Dubois[1,2,3], Yves Coudière[1,4,5], Mark Potse[1,4,5]

[1] IHU Liryc, Electrophysiology and Heart Modeling Institute, F-33000 Pessac, France
[2] Univ. Bordeaux, CRCTB, U1045, Bordeaux, France
[3] INSERM, CRCTB, U1045, Bordeaux, France
[4] CARMEN Research Team, INRIA, Bordeaux, France
[5] Bordeaux University, IMB UMR 5251, F-33400 Talence, France
gwladys.ravon@ihu-liryc.fr

Abstract. The main challenge of electrocardiography is to retrieve the best possible electrical information from body surface electrical potential maps. The most common methods reconstruct epicardial potentials. Here we propose a method based on a parameter identification problem to reconstruct both activation and repolarization times. The shape of an action potential (AP) is well known and can be described as a parameterized function. From the parameterized APs we compute the electrical potentials on the torso. The inverse problem is reduced to the identification of all the parameters. The method was tested on *in silico* and experimental data, for single ventricular pacing. We reconstructed activation and repolarization times with good accuracy accurate (CC between 0.71 and 0.9).

1 Introduction

The main challenge of electrocardiography is to retrieve the best possible electrical information from body surface electrical potential maps (BSPM). The most common approach relies on the inverse solution of the Laplace equation in the torso. It reconstructs epicardial potential maps from the BSPM. This technique requires a regularization strategy to deal with the ill-posedness of the problem, and a discretization method to approximate the Laplace equation. A Tikhonov regularization and the Method of Fundamental Solutions (MFS) are commonly used, as proposed by Wang and Rudy [1]. Relevant activation maps can be retrieved from this inverse solution, though it provides signals with a lower amplitude. Nevertheless the reconstruction of accurate activation maps and repolarization maps remains a very challenging problem.

Alternative formulations have been proposed Liu *et al.* [2] and by Van Oosterom *et al.* [3], in order to reconstruct directly the activation times (ATs). The method proposed by Liu *et al.* looks for the three-dimensional activation sequence in the ventricular muscle. The method of Van Oosternom *et al.* considers both epicardium and endocardium. These approaches still rely on a regularization technique and are not designed to obtain repolarization maps.

We introduce a new technique that aims at recovering both the activation and repolarization maps on the epicardium. We first focus on single ventricular pacing cases. We propose an approach based on a parameter identification (PI) problem. As epicardial potentials are difficult to parameterize, we rather represent the action potential (AP) as a function of 4 parameters; namely the amplitude, activation time, plateau phase duration and repolarization slope. The final parameter identification problem consists of identifying these 4 space-dependent parameters from the complete BSPM sequence. This method solves the whole electrical sequence: depolarization and repolarization. Since it introduces *a priori* the shape of the AP, no regularization is needed. The nonlinear least squares parameter identification problem is solved by a gradient method.

The method was tested on both *in silico* and *ex vivo* experimental data. We found that activation maps from PI were at least as good as those from the MFS. Accuracy of reconstructed repolarization maps and torso potentials were also discussed.

2 Methods

2.1 Parameterization of the action potential

Following the work of Van Oosterom [4] we define the transmembrane potential (TMP) as the function:

$$V_{\mathrm{m}}(t,x) = \mathcal{A}\mathcal{F}(\alpha, t - \tau)\mathcal{F}(-\alpha_{\mathrm{R}}, t - (\tau + \tau_{\mathrm{R}})), \tag{1}$$

where $\mathcal{F}(\alpha, \zeta) = \dfrac{1}{1 + \exp^{-\alpha\zeta}}$. α is the constant slope of the depolarization. Its value (3.3 ms^{-1}) is taken from the same study [4]. $\mathcal{A}$ is the amplitude, τ the activation time, τ_{R} the plateau phase duration and α_{R} the slope of the repolarization (see Figure 1). Each of these 4 parameters may be space-dependent. Note that in our study the amplitude does not have physiological value. It is a qualitative parameter made to fit the amplitude of the given BSPM.
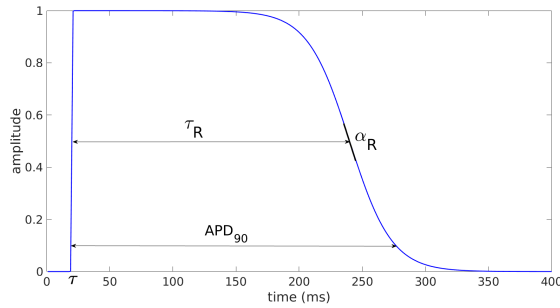
Fig. 1. Parameterized action potential with $\tau = 20$ms and $\tau_{\mathrm{R}} = 220$ms.

2.2 Mapping the TMP to the BSPM

Given the TMP V_m on each point x_j of the epicardium, we compute the extra-cellular potentials:

$$\phi_\mathrm{e}(x_j, t) = \overline{V_\mathrm{m}}(t) - V_\mathrm{m}(x_j, t) \quad j = 1, \dots, N_\mathrm{H}, \tag{2}$$

where N_H is the number of points on the heart surface. $\overline{V_\mathrm{m}}(t)$ is the spatial mean of V_m at each time. This formulation is derived from the monodomain model [5].

Finally, we approximate the solution of the Laplace equation far from the heart surface by [6,7]:

$$\phi_\mathrm{T}(y, t) = \sum_{j=1}^{N_\mathrm{H}} \frac{1}{4\pi \|x_j - y\|} \phi_\mathrm{e}(x_j, t), \tag{3}$$

where y is any point on the body surface. These ϕ_T will be compared to the BSPM.

2.3 The parameter identification problem

As a consequence we look for the parameter set $\mathcal{P} = (\mathcal{A}, \tau, \tau_\mathrm{R}, \alpha_\mathrm{R})$ that minimizes the least squares error

$$J(\mathcal{P}) = \frac{1}{2} \sum_{k=k_1}^{k_2} \sum_{i=1}^{N_\mathrm{T}} (\phi_\mathrm{T}(y_i, t_k) - \phi^\star(y_i, t_k))^2, \tag{4}$$

where $(y_i)_{i=1 \dots N_\mathrm{T}}$ are the N_T electrode locations on the body surface, $(t_k)_{k=k_1 \dots k_2}$ is the time sequence of interest, and $(\phi^\star(y_i, t_k))$ are the measured BSPM.

However, in order to improve the convergence of the method we make the following choices:

- the amplitude and the repolarization slope are set to a constant over the whole epicardium
- τ and τ_R are space-dependent. $(\tau_j)_j$ and $(\tau_{\mathrm{R},j})_j$ are taken at the same location on the epicardium as $(x_j)_j$
- the parameter set is split into the depolarization subset $\mathcal{P} = (\mathcal{A}, (\tau_j)_j)$ and the repolarization subset $\mathcal{P} = ((\tau_\mathrm{R})_j, \alpha_\mathrm{R})$.

During the depolarization phase of a paced or normal beat we can assume that $t \ll \tau + \tau_\mathrm{R}$, so that $V_\mathrm{m}(t, x) \simeq \mathcal{A} \mathcal{F}(\alpha, t - \tau)$. Hence we solve for $\mathcal{P} = (\mathcal{A}, (\tau_j)_j)$ in (4) on a time interval $[t_{k_1}, t_{k_2}]$ that covers the total QRS interval, but contains no T wave (see Figure 2). Still in order to improve the convergence, we split the identification in two steps: we first identify the constant amplitude $\mathcal{A}$, and then the ATs $(\tau_j)_j$. We apply a standard MFS with a regularization method [1]. This

gives us electrical potentials on the heart surface. We then compute the ATs as the time with the highest negative slope. When we identify the amplitude the parameter set $\mathcal{P}$ is simply the singleton $\{\mathcal{A}\}$, and ATs obtained from the MFS are an input in our PI problem. Once we have this optimized amplitude $\mathcal{A}^\star$ it becomes an input and the cost function J is minimized for $\mathcal{P} = ((\tau_j)_j)$.

During the repolarization phase, we solve for $\mathcal{P} = ((\tau_{R,j})_j, \alpha_R)$ in (4) on a time interval $[t_{k_1}, t_{k_2}]$ that covers the total extent of the T waves (see Figure 2). We first identify the constant slope (e. g. $\mathcal{P} = (\alpha_R)$). The input plateau phase durations are coarsely determined from the given BSPM. Once we have the optimum $\alpha_R^\star$ we minimize J for $\mathcal{P} = ((\tau_{R,j})_j)$. Optimum $\mathcal{A}^\star, (\tau_j^\star)_j$ and $\alpha_R^\star$ are an input in this PI problem.
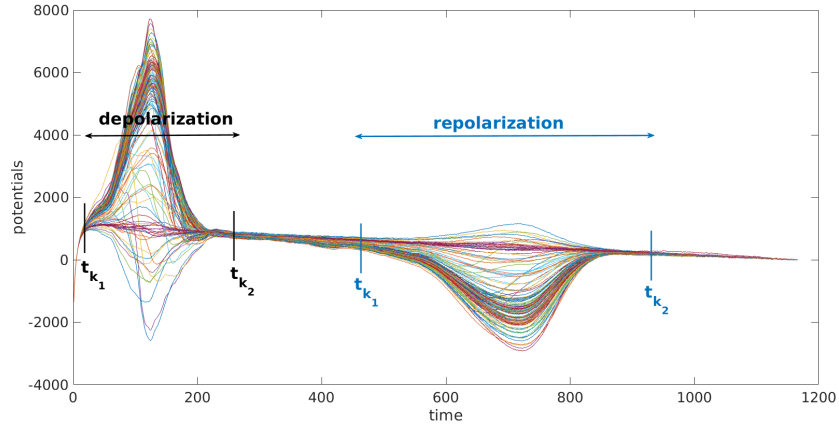
Fig. 2. Example of choice for k_1 and k_2 for experimental signals. Each curve represents the signal of one of the torso electrodes.

These four nonlinear least squares problems are solved by the gradient descent method. The explicit gradient of the cost function J with respect to the unknown parameters $\mathcal{P}$ is calculated analytically. If we wait for the method to converge overfitting occurs. It means that there are small changes in the cost function but the quality of the activation map decreases. To avoid overfitting, we couple the gradient descent method with an early stopping criterion based on the shape of the learning curve. For each gradient descent method, an initial guess is required. For the amplitude, we obtain this guess manually with a dichotomy approach. For the ATs, we use the ATs computed from the MFS. The initial guess for the slope is arbitrarily set to 1. The overall algorithm is summarized below.

Algorithm 1.1

   Depolarization phase

1: Standard MFS on interval $[t_{k_1}, t_{k_2}]$
2: Compute ATs from MFS solution
3: Gradient descent to optimize the amplitude (MFS ATs as input)
4: Gradient descent to optimize the ATs (optimum $\mathcal{A}^\star$ as input)
5: Gradient descent to optimize the amplitude (optimum $\tau^\star$ as input)

   Repolarization phase

1: Input: $\mathcal{A}^\star$ and $\tau^\star$, from torso signal for τ_R
2: Gradient descent to optimize the constant slope α_R
3: Gradient descent to optimize the $(\tau_{R,j})_j$ (optimum $\alpha_R^\star$ as input)
4: Gradient descent to optimize the slope (optimum $\tau_R^\star$ as input)

---

3 Results

3.1 *In silico* data

In order to create *in silico* testing data, a simulation was run on an anatomically realistic 3D geometry of the torso, including heart, blood vessels, lungs and skeletal muscle. Each organ had its own conductivity. Propagating action potentials were generated using a monodomain reaction-diffusion model with a Ten Tusscher membrane model [8]. An anisotropic human heart model at 0.2mm resolution was used for this purpose. An anisotropic Laplace equation was solved in the torso volume with a finite difference method [9]. We had access to the transmembrane potentials on the subepicardium and extra-cellular potentials on the epicardium. ATs were calculated from the epicardial potentials with the same method as the ATs from the MFS solution. Repolarization times were computed from epicardial potentials as the time with the highest positive slope during the repolarization phase.
On the same model anatomy, two different simulations were run: a left ventricular (LV) pacing, and a right ventricular (RV) one. For both cases, we identified our parameters following the algorithm detailed in Algorithm 1.1.

We first looked at the ATs. For the LV pacing the method converged to satisfactory ATs on the whole heart (Figure 3, left). Our method gave a better range of ATs than the MFS. However for both methods the pacing site was not well localized. For the RV pacing, late activations were better reconstructed than the early ones. The correlation coefficient (CC) was the same for both methods but the distribution of points in the scatter plots was different. Indeed for the MFS we observed clustering of points along horizontal lines. This means that there were discontinuities in the distribution of ATs. These discontinuities were not consistent with the reference ATs (Figures 3, right and 4). On the map on the right, discontinuities are clearly visible between the dark blue and light green parts and between the dark green and orange parts.
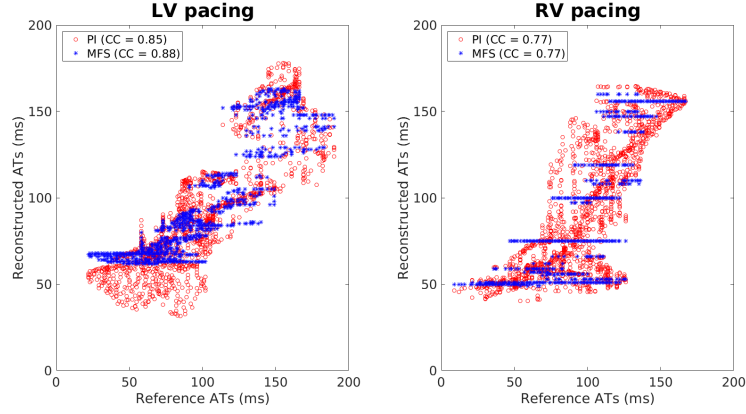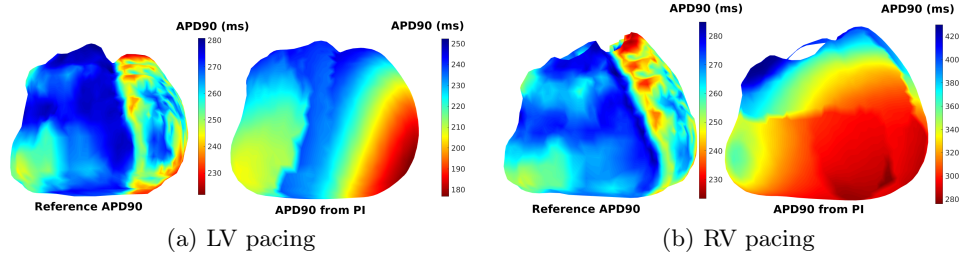
Fig. 3. Scatter plot of the ATs for *in silico* data. For each point, the x coordinate is the reference AT and the y coordinate is the corresponding reconstructed AT (PI in red, MFS in blue).
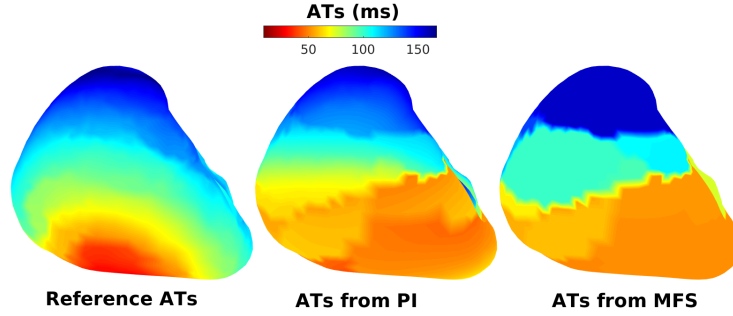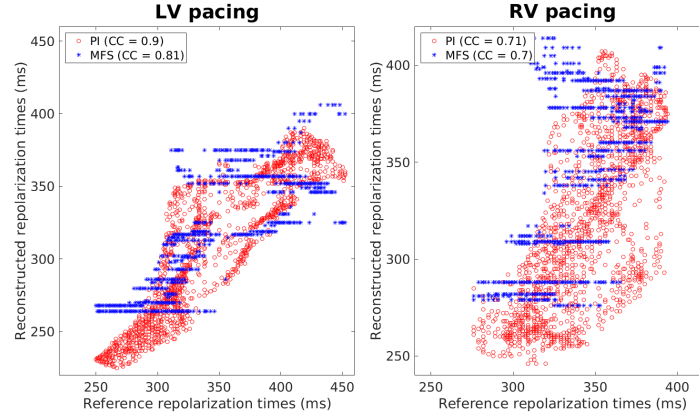

Fig. 4. Activation maps of the RV pacing *in silico* case.

In Figure 5 we compare APD90 calculated from the reference APs and from the reconstructed ones, for both LV and RV pacing. First of all, we had a larger range of APD90 from the PI, especially for the RV pacing. Moreover, there was a clear difference in the repartition of APD90 between the LV and the RV. This difference was not correctly reconstructed with the PI approach.

We compare the repolarization times in Figure 6. For the PI, the CC were 0.9 and 0.71 for the LV and RV pacing, respectively. These values were close to those for the MFS but we observed discontinuities in the distribution of points, as for the ATs (see Figure 7). Note that the quality of the reconstruction from the PI method was better for the repolarization times than for the APD90. This can be explained by the fact that if we had an error in the parameter τ, it would imply another error in the parameter τ_R to fit the repolarization phase correctly.

(a) LV pacing (b) RV pacing

Fig. 5. Comparison of APD90. The reference APD90 are obtained on the subepi-cardium mesh and the reconstructed APD90 on the epicardium mesh. Anteroposterior view.


Fig. 6. Scatter plot of the repolarization times for *in silico* data.
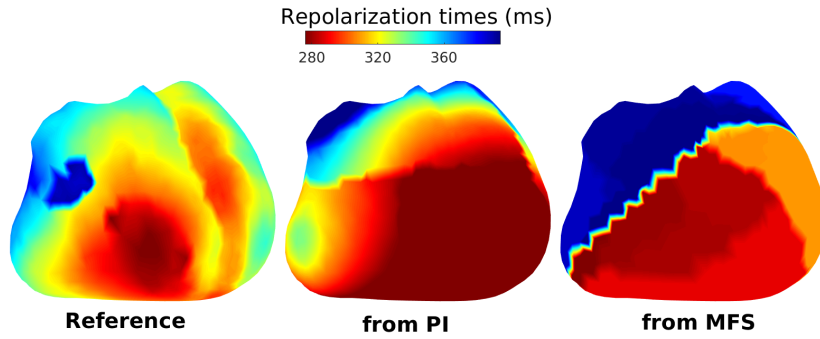
Fig. 7. Repolarization maps of the RV pacing *in silico* case.

Finally we compare signals on the torso. Reconstructed potentials were computed from equations (1), (2) and (3) with the optimized parameters. In both cases the amplitude was optimized to fit the given BSPM. Figure 8 shows given and reconstructed potentials on two torso electrodes. For the LV pacing the amplitude of the signal was better fitted on the first electrode than on the second. Both depolarization and repolarization phases were quite well identified. These two electrodes were representative for the 252 torso electrodes. For the RV pacing, on the same electrodes, the reconstruction was less accurate. Specifically, the repolarization was inverted on the first electrode, while on the second the depolarization was. This was due to the incorrect activation times on the right ventricle. In this case, the chosen electrodes exhibit some of the worst reconstructed potentials.


(a) LV pacing   (b) RV pacing
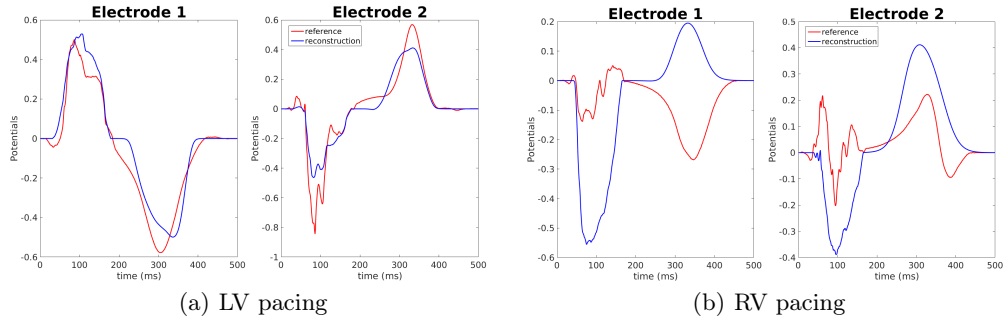
Fig. 8. Reconstructed potentials for *in silico* data. Electrode 1: close to the heart, Electrode 2: right hip. Red line: reference BSPM; blue line: reconstructed BSPM.
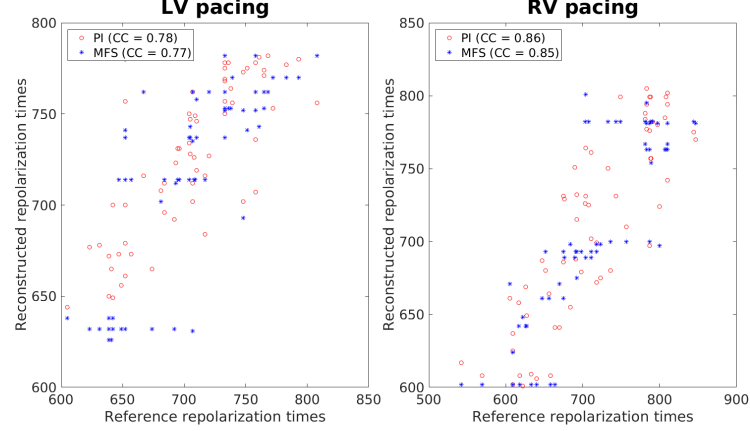
3.2 Experimental data

Experimental data were obtained from a Langendorff-perfused pig heart with an oxygenated electrolytic solution. Epicardial potentials were recorded with a flexible electrode sock (108 electrodes) placed over the epicardium. The heart was placed inside a human-shaped tank. BSPM were recorded from 128 electrodes, simultaneously with epicardial potentials. LV and RV pacing were performed with 1 Hz frequency. We removed signals from bad leads (e.g. not well connected) and the baseline. Finally we made a signal averaging over the whole recording to obtain a single beat.

We first looked at the ATs. As for the *in silico* data, it was difficult to localize the pacing sites precisely. Nevertheless the reconstructed ATs were satisfactory (Figure 9). We noticed a slight improvement of our method compared to MFS for the LV pacing (CC: 0.85 vs 0.82). On the RV pacing (CC: 0.92 vs 0.89) improvement was more obvious when we compared the distribution of points.
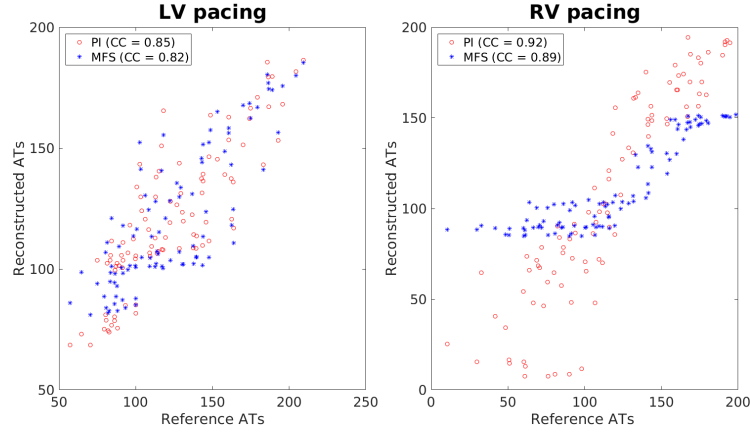
Fig. 9. Scatter plot of the ATs for experimental data

Scatter plots of the repolarization times are presented in Figure 10. For both cases, the reconstructed repolarization phase was shorter than the real. The CC were very close for the PI and the MFS but with the PI the distribution was smoother.

Fig. 10. Scatter plot of the repolarization times for experimental data.

Reconstructed potentials are presented in Figure 11. With our method we were able to identify both depolarization and repolarization phases. The amplitude of the signals was well reproduced thanks to the optimized amplitude $\mathcal{A}^{\star}$. We did not have any inversions of the T wave. The chosen electrodes were representative for all the electrodes.

(a) LV pacing   (b) RV pacing
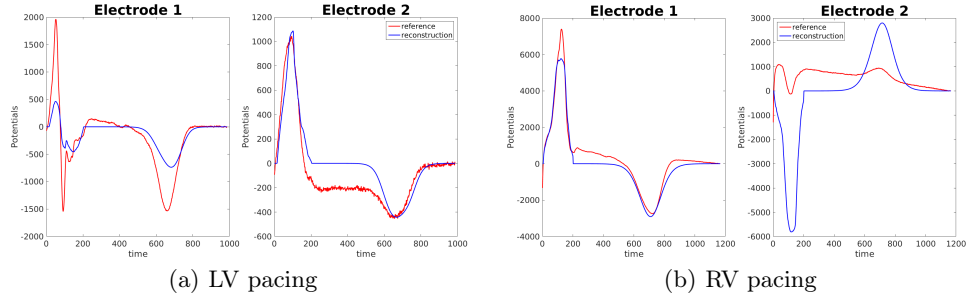
Fig. 11. Reconstructed potentials for experimental data. Electrode 1: close to the heart, Electrode 2: right hip. Red line: reference BSPM; blue line: reconstructed BSPM

4 Conclusion

We presented a parameter optimization method to solve the inverse problem of electrocardiography. Our method relies on a parameterization of the AP. Our main objective was to develop a method that gives precise information on the repolarization phase, in addition to information on the depolarization phase. Moreover, this approach gives access to all the properties of a local AP, like APD90.

We had to make some choices to ensure a good convergence and avoid overfitting: constant amplitude and slopes; split the identification process in two steps. Compared to the MFS, our PI gave better activation maps: we obtained a better range of ATs and did not have any artificial discontinuities in the distribution of the ATs on both *in silico* and experimental data. The method fitted the repolarization phases quite accurately. However, having a good fit on the repolarization time could hide an error in the plateau phase duration. Indeed an error in the AT would lead to an error in the plateau phase duration to fit the repolarization phase. Reconstructed torso potentials were close to the measured ones. Especially, optimized amplitude enabled to fit BSPM amplitudes. Moreover, both depolarization and repolarization phases were well caught on all the torso.

To improve the quality of the results, we plan to add either the septum or the endocardium into the geometry. Another development will be to consider piecewise constant amplitudes and repolarization slopes, instead of constant over the whole epicardium.

Acknowledgments

References

1. Y. Wang, Y. Rudy: Application of the method of fundamental solutions to potential-based inverse electrocardiography. Ann. Biomed. Eng. 2006; 34:1272-1288
2. Z. Liu, C. Liu, B. He: Noninvasive reconstruction of three-dimensional ventricular activation sequence from the inverse solution of distributed equivalent current Density. IEEE Trans. Med. Imag., vol 25, 1307-1318 (2006)
3. A. van Oosterom, T. Oostendorp: On computing pericardial potentials and current densities in inverse electrocardiography. J. Electrocardiol. 25S:102–106 (1993)
4. A. van Oosterom, V. Jacquemet: A parameterized description of transmembrane potentials used in forward and inverse procedures. Int. Conf. Electrocardiol. 6, 5-8 (2005)
5. S. Labarthe: Modélisation de l'activité électrique des oreillettes et des veines pulmonaires. Thesis, University of Bordeaux (2013)
6. J. Malmivuo, R. Plonsey: Bioelectromagnetism: principles and applications of bioelectric and biomagnetic fields. Oxford University Press, USA (1995)
7. P. W. Macfarlane, A. van Oosterom, O. Pahlm, P. Kligfield, M. Janse, J. Camm: Comprehensive Electrocardiology. Springer London (2010)
8. K. H. W. J. ten Tusscher, D. Noble, P. J. Noble, A. V. Panfilov: A model for human ventricular tissue. Am. J. Physiol. H., vol 286 (2004)
9. M. Potse, B. Dubé, A. Vinet: Cardiac anisotropy in boundary-element models for the electrocardiogram. Med. Biol. Eng. Comput., 47(7), 719-729 (2009)